Investigation of wired and wireless services based on OFDM DSB-RC transmission in the presence of modulation chirp of a DEMZM

Paulo Almeida[1,*] and Henrique Silva[1,2]

[1]*Instituto de Telecomunicações, Department of Electrical and Computer Engineering, University of Coimbra, Coimbra 3030-290, Portugal*

[2]*hjas@co.it.pt*

**palmeida@co.it.pt*

Abstract: In this paper, we investigate the performance of intensity modulation with optical carrier reduced by biasing a dual-electrode Mach-Zehnder modulator (DEMZM) below its quadrature point, in the presence of controlled modulation chirp. The effects of the modulation chirp and of the bias point of a DEMZM on the received signal are analytically derived for small-signal operation. The interaction of these two effects is assessed in terms of optical signal to noise ratio (OSNR) required for a BER = 10^{-9}, through a comparison between double sideband (DSB) modulation and double sideband - reduced carrier (DSB-RC) modulation, by numerical simulation. We found that the power of the optical carrier has impact on the optimum value of the α chirp parameter and that a positive value of the α chirp parameter can be the optimum value to drive a DEMZM, depending on the central frequency of the orthogonal frequency division multiplexing (OFDM) signal and on the DEMZM bias point.

OCIS codes: (060.2330) Fiber optics communications; (060.4080) Modulation.

References and links

1. M. Popov, "The convergence of wired and wireless services delivery in access and home networks" *Proc. Optical Fiber Communication conference* (2010), paper OWQ6.
2. X. Mazda and F. Mazda, *Focal Illustrated Dictionary of Telecommunications* (Focal Press, 2013).
3. R. Hui, Z. Benyuan, H. Renxing, C. T. Allen, K. Demarest, and D. Richards, "Subcarrier multiplexing for high-speed optical transmission," J. Lightwave Technol. **20**(3), 417–427 (2002).
4. M. Attygalle, C. Lim, G. J. Pendock, A. Nirmalathas, and G. Edvell, "Transmission improvement in fiber wireless links using fiber Bragg gratings," IEEE Photon. Technol. Lett. **17**(1), 190–192 (2005).
5. J. Leibrich, A. Ali, H. Paul, W. Rosenkranz, and K. D. Kammeyer, "Impact of modulator bias on the OSNR requirement of direct-detection optical OFDM," IEEE Photon. Technol. Lett. **21**(15), 1033–1035 (2009).
6. P. Almeida and H. Silva, "Impact of the modulation chirp of a DEMZM on the transmission of signals based on OFDM," IEEE Photon. Technol. Lett. **25**(3), 283–286 (2013).
7. J. L. Wei, E. Hugues-Salas, R. P. Giddings, X. Q. Jin, X. Zheng, S. Mansoor, and J. M. Tang, "Wavelength reused bidirectional transmission of adaptively modulated optical OFDM signals in WDM-PONs incorporating SOA and RSOA intensity modulators," Opt. Express **18**(10), 9791–9808 (2010).
8. D. Z. Hsu, C. C. Wei, H. Y. Chen, J. Chen, M. C. Yuang, S. H. Lin, and W. Y. Li, "21 Gb/s after 100 km OFDM long-reach PON transmission using a cost-effective electro-absorption modulator," Opt. Express **18**(26), 27758–27763 (2010).
9. H. Silva, R. Fyath, and J. O'Reilly, "Sensitivity degradation with laser wavelength chirp for direct-detection optical receivers," IEE Proc. Optoelectron.– Pt. J,**136**(4), 209–218, (1989).
10. C. Sánchez, B. Ortega, J. L. Wei, J. Tang, and J. Capmany, "Analytical formulation of directly modulated OOFDM signals transmitted over an IM/DD dispersive link," Opt. Express **21**(6), 7651–7666 (2013).
11. P. Almeida and H. Silva, "Expressions of the chirp parameter components for intensity modulation with a dual-electrode Mach-Zehnder modulator, " *Proc. International Conference on Transparent Optical Networks* (2012).
12. S. Walklin and J. Conradi, "Effect of Mach-Zehnder modulator DC extinction ratio on residual chirp-induced dispersion in 10-Gb/s binary and AM-PSK duobinary lightwave systems," IEEE Photon. Technol. Lett. **9**(10), 1400–1402 (1997).
13. P. Almeida and H. Silva, "Corrections to "Impact of the modulation chirp of a DEMZM on the transmission of signals based on OFDM," IEEE Photon. Technol. Lett. **25**(11), 1087–1087 (2013).
14. G. P. Agrawal, *Fiber-Optic Communication Systems*, (NJ, 2002).

#196157 - $15.00 USD Received 20 Aug 2013; revised 4 Nov 2013; accepted 21 Nov 2013; published 6 Dec 2013

15. L. V. T. Nguyen and D. B. Hunter, "A photonic technique for microwave frequency measurement," IEEE Photon. Technol. Lett. **18**(10), 1188–1190 (2006).
16. *High rate ultra wideband PHY and MAC standard* (2007). European Computer Manufacturers Association International Std. ECMA-368.
17. A. B. Carlson, P. B. Crilly, and J. C. Rutledge, *Communications systems- An introduction to signals and noise in electrical communication,* (Mc Graw-Hill, 2002).
18. A. Ali, J. Leibrich, and W. Rosenkranz, "Spectral efficiency and receiver sensitivity in direct detection optical-OFDM,*" Proc. Conference on Optical Fiber Communication conference* (2009), paper OMT7.
19. W. Peng, K. Feng, A. E. Willner, and S. Chi, "Estimation of the bit error rate for direct-detected OFDM signals with optically preamplified receivers," IEEE/OSA J. Lightwave Technol. **27**(10), 1340–1346 (2009).
20. T. Alves and A. Cartaxo, "Analysis of methods of performance evaluation of direct-detection OFDM communication systems," Fiber Integr. Opt. **29**(3), 170–186 (2010).
21. T. Dennis and P. A. Williams, "Chirp characterization of external modulators with finite extinction ratio using linear optical sampling," IEEE Photon. Technol. Lett. **22**(9), 646–648 (2010).
22. F. Devaux, Y. Sorel, and J. F. Kerdiles, "Simple measurement of fiber dispersion and of chirp parameter of intensity modulated light emitter," J. Lightwave Technol. **11**(12), 1937–1940 (1993).
23. M. Morant, T. Alves, A. Cartaxo, and R. Llorente, "Transmission impairment compensation using broadband channel sounding in multi-format OFDM-based long-reach PONs," *Proc. Optical Fiber Communication Conference,*(2012), paper OW3B.2.

1. Introduction

Convergence of wired and wireless access networks into a single hybrid optical access infrastructure based on radio-over-fiber (RoF) networks has gained considerable momentum in recent years, due to the possibility of offering the final user a single simplified access to broadband services. Furthermore, the merging of two different access networks allows reducing upgrade and management costs of future broadband access networks [1]. This convergence, applied on long-reach passive optical networks (LR-PONs), allows reducing the network cost of operation further, since a larger geographic area can be covered with a single central office (CO) and without optical-electrical-optical conversions at the middle of the network.

Intensity modulation direct-detection (IMDD) systems are largely used in optical access networks due to their simplicity and reduced cost. However, IMDD systems present some drawbacks, such as power fading induced by chromatic dispersion, which occurs after photodetection due to the inherent double sideband (DSB) spectrum, and low modulation efficiency, since at least 50% of the optical power is wasted in the optical carrier, which does not carry any information.

To overcome the latter drawback, the modulation efficiency has been improved with double sideband - reduced carrier (DSB-RC) modulation [2], obtained by reducing the power of the optical carrier with an optical notch filter, such as a Fabry-Pérot filter in reflection mode [3] or a narrow band fiber Bragg grating [4]. More recently, a cost-effective method based on biasing the Lithium Niobate (LiNbO3) Mach-Zehnder modulator (MZM) below its quadrature point (QP), to reduce the power of the optical carrier, has been demonstrated [5].

To mitigate the former drawback, the power fading induced by chromatic dispersion in orthogonal frequency division multiplexing (OFDM) IMDD systems, the introduction of controlled negative modulation chirp by a dual electrode MZM (DEMZM) has been shown to mitigate the dispersion penalty [6]. Up to now, the transmission of optical signals in the presence of modulation chirp has been demonstrated only for intensity modulated signals with full optical carrier, through DEMZMs [6], semiconductor optical amplifiers [7], electro-absorption modulators [8], or laser diodes [9, 10]. In [11], it has been analytically demonstrated that, inside a bias voltage range around the QP of a DEMZM, the expressions derived for the α chirp parameter components can be used to estimate the modulation chirp, whereas at the maximum transmission point (MATP) or minimum transmission point (MITP) of the intensity transfer function of the DEMZM the expressions derived are not valid due to singularities in the expression of the α chirp parameter. Unlike the other aforementioned devices, the expression of the α chirp parameter of the DEMZM does not depend on the average optical power, *i.e.* power of the optical carrier. This opens the possibility of improving the modulation efficiency of IMDD systems, by employing DSB-RC modulation

#196157 - $15.00 USD Received 20 Aug 2013; revised 4 Nov 2013; accepted 21 Nov 2013; published 6 Dec 2013

along with controlled modulation chirp to mitigate the power fading induced by chromatic dispersion.

In this paper, we investigate analytically and numerically the performance obtained with an optical hybrid signal (OHS) composed by a custom OFDM Gigabit Ethernet (OFDM-GbE) signal and three independent OFDM ultra-wideband (OFDM-UWB) signals, when modulation chirp is introduced in the intensity modulation with reduced carrier based on a DEMZM. The optical carrier is reduced by biasing the DEMZM below its QP, in a bias point determined as the best value for all signals considered.

The remainder of this paper is organized as follows. A mathematical description of the effect of modulation chirp on the received signal and the effect of the DEMZM bias point on the modulation efficiency is presented in Section 2. In Section 3, the modeling of a wavelength division multiplexed passive optical network (WDM-PON) operating with a single wavelength is described, based on the equivalent block diagram of the system used to evaluate the performance obtained with the received OHS, when transmitted in the presence of modulation chirp. In the same section, the main parameters required to generate the baseband OFDM signals are presented. The numerical simulation results comparing the effect of modulation chirp on DSB and DSB-RC modulations are presented in Section 4, and the main specifications required to drive the DEMZM and limitations of the transmission system found are pointed out. Finally, in Section 5 the main conclusions of this work are drawn.

2. Theoretical analysis

2.1 Effect of modulation chirp of a DEMZM on the received signal

A complex-valued baseband OFDM signal up-converted to the central frequency, f_{rf} ($\omega_{rf} = 2\pi f_{rf}$), can be expressed by:

$$x(t) = x_i(t)\cos(\omega_{rf} t) - x_q(t)\sin(\omega_{rf} t) \tag{1}$$

where $x_i(t)$ and $x_q(t)$ are the baseband in-phase and quadrature components of the OFDM signal with zero mean and energy σ^2_{xi} and σ^2_{xq}, respectively, at the output of the OFDM modulator, before the RF up-converter. The optical field at the output of the LiNbO3 DEMZM with finite extinction ratio (ER) can be expressed by [12]:

$$E_{MZM}(t) = \frac{\sqrt{2P}e^{j\omega_c t}}{2}\left\{ e^{j\frac{\pi}{V_\pi}(V_1 x(t) - V_{bias1})} + \gamma e^{j\frac{\pi}{V_\pi}(V_2 x(t) + V_{bias2})} \right\}, \tag{2}$$

where the amplitude drive voltages for any value of the α chirp parameter are expressed as [13]:

$$V_1 = 2\frac{\gamma\cos(\pi V_{bias}/V_\pi) + \gamma^2 - \alpha\gamma\sin(\pi V_{bias}/V_\pi)}{2\gamma\cos(\pi V_{bias}/V_\pi) + 1 + \gamma^2} m V_\pi \tag{3}$$

$$V_2 = -2\frac{\gamma\cos(\pi V_{bias}/V_\pi) + 1 + \alpha\gamma\sin(\pi V_{bias}/V_\pi)}{2\gamma\cos(\pi V_{bias}/V_\pi) + 1 + \gamma^2} m V_\pi \tag{4}$$

where $V_{bias} = -(V_{bias1} + V_{bias2})$ is the bias voltage of the DEMZM, determined by the DC voltages V_{bias1} and V_{bias2}, V_π is the half-wave voltage of the DEMZM, m is the modulation index, P is the average power of the continuous wave (CW) laser emitting at the frequency v_c ($\omega_c = 2\pi v_c$) fed into the optical input of the DEMZM, and γ is the scaling factor, between 0 and 1, used to account for the unbalance between the arms and related with the ER of the DEMZM [12]. For balanced DEMZMs, this scaling factor is 1. Under small-signal modulation conditions ($m << 1$), the higher order sidebands are small and can be ignored, and thus the optical field signal given by Eq. (2) can be simplified to:

#196157 - $15.00 USD Received 20 Aug 2013; revised 4 Nov 2013; accepted 21 Nov 2013; published 6 Dec 2013

$$E_{MZM}(t) \cong \frac{\sqrt{2P}}{2}\left\{E_{-}e^{j(\omega_c-\omega_{rf})t} + E_0 e^{j\omega_c t} + E_{+}e^{j(\omega_c+\omega_{rf})t}\right\}, \quad (5)$$

with

$$\begin{aligned} E_{-} &= -\left[\Gamma_1\Lambda_1^{*} + \gamma\Gamma_2\Lambda_2^{*})\right] \\ E_0 &= \left[\Gamma_1 A_1 + \gamma\Gamma_2 A_2)\right] \\ E_{+} &= \left[\Gamma_1\Lambda_1 + \gamma\Gamma_2\Lambda_2)\right] \end{aligned} \quad (6)$$

with $\Gamma_1 = \exp(-j\pi V_{bias1}/V_\pi)$, $\Gamma_2 = \exp(j\pi V_{bias2}/V_\pi)$, $\Lambda_k = J_1(\theta_{kq}(t)) + jJ_1(\theta_{ki}(t))$, $A_k = J_0(\theta_{ki}(t)) + J_0(\theta_{kq}(t))$, where $J_n(\cdot)$ is the Bessel function of the first kind and order n (n = 0,1), and $\theta_{ki}(t) = \pi V_k x_i(t)/V_\pi$, $\theta_{kq}(t) = -\pi V_k x_q(t)/V_\pi$ are the modulation phase shifts of the baseband in-phase and quadrature components, respectively, when applied to the electrode k = 1,2. The superscript * denotes the complex conjugate and $j = \sqrt{-1}$ .When this optical signal is transmitted over a dispersive single mode fiber, a phase shift is induced into each optical sideband, relative to the optical carrier. The Taylor's expansion of the dispersion propagation constant of the dispersive fiber can be expressed as [14]:

$$\beta(\omega) \approx \beta_0 + \beta_1(\omega-\omega_c) + \beta_2/2(\omega-\omega_c)^2, \quad (7)$$

where $\beta_m = d^m\beta(\omega)/d\omega^m|_{\omega=\omega_c}$. The effect of higher order fiber dispersion at 1550 nm is neglected. For the sideband centered at the frequency $\omega_c \pm \omega_{rf}$, the dispersion propagation constant is given by:

$$\beta(\omega_c \pm \omega_{rf}) = \beta_{\pm} = \beta_0 \pm \beta_1\omega_{rf} + \beta_2/2\,\omega_{rf}^2. \quad (8)$$

After transmission over a standard single-mode fiber (SSMF) of length L, the optical field can be written as:

$$E(t,L) \cong \frac{\sqrt{2P}}{2}\left\{E_{-}e^{-j\beta_{-}L}e^{j(\omega_c-\omega_{rf})t} + E_0 e^{-j\beta_0 L}e^{j\omega_c t} + E_{+}e^{-j\beta+L}e^{j(\omega_c+\omega_{rf})t}\right\}. \quad (9)$$

Considering a limited bandwidth positive-intrinsic-negative (PIN) photodiode with responsivity $\Re$, the photocurrent is expressed as:

$$i(t) = \Re\left\{E(t,L)E(t,L)^{*}\right\} = i_{DC} + i_s(t) \quad (10)$$

where i_{DC} the DC photocurrent and $i_s(t)$ the signal photocurrent. Considering the small-signal approximation, $J_n(x) \approx 1/n!(x/2)^n$, we derived the following expression for the signal photocurrent as a function of the system parameters:

$$i_s(t) \approx 2\Re P\pi\gamma m F_{bias}\sqrt{1+\alpha^2}\cos\left(\frac{\pi D\lambda_c^2 f_{rf}^2 L}{c} + \arctan(\alpha)\right)\left[x_i(t) + jx_q(t)\right]\cos\left(\omega_{rf}(t-\tau)\right) \quad (11)$$

where $F_{bias} = \sin(\pi(V_{bias1} + V_{bias2})/V_\pi)$, D is the dispersion parameter, λ_c is the carrier wavelength, and $\tau = \beta_1 L$ is the time delay suffered by the optical signal propagating a distance L through optical fiber with a group delay per unit length β_1. In the derivation of Eq. (11), a very narrow-bandwidth OFDM signal was assumed, such that the amplitude factor cos(·) present in Eq. (11) for the central frequency f_{rf} can be assumed constant over all the signal bandwidth. It should be noted that, in the case of a real-valued OFDM signal, the expression of Eq. (11) continues valid, with $x_q(t) = 0$.

The average power of the photodetected signal can be approximated by:

#196157 - $15.00 USD Received 20 Aug 2013; revised 4 Nov 2013; accepted 21 Nov 2013; published 6 Dec 2013

$$P_{rf} = \langle i_s(t)^2 \rangle R_L \approx 2R_L \left(\Re P \pi \gamma m\right)^2 F_{bias}^2 \left(\sigma_{xi}^2 + \sigma_{xq}^2\right)\left(1+\alpha^2\right)\cos\left(\frac{\pi D \lambda_c^2 f_{rf}^2 L}{c} + \arctan(\alpha)\right)^2 \quad (12)$$

where $\langle \cdot \rangle$ denotes the averaging operator in the time domain and R_L is the load resistor where the RF power is measured. The RF power given by Eq. (12) is in accordance with Eq. (1) in [15], when normalized by the RF power in optical back-to-back (B2B) configuration, considering as modulating signal a real sinusoidal signal ($x_q(t) = 0$). Thus, Eq. (12) is the general expression of the RF power after photodetection, in the presence of the modulation chirp. From Eq. (12) we can conclude that: (1) When the DEMZM is biased at its null intensity point, (V_{bias1} and V_{bias2} equal to $V_\pi/2$), there is no signal photocurrent located at the frequency ω_{rf};this is clear since, in this case, at the output of the DEMZM only odd-order harmonics of ω_{rf} are present, and there is no optical carrier to beat with the 1st order harmonics to generate the photocurrent signal at ω_{rf}. (2) The negative values of the chirp parameter factor arctan(α), within the argument of the cosine function, have the effect of generating a phase shift opposite to that caused by the cumulative dispersion along the fiber; thus, the first null occurs for a greater fiber length in the presence of negative chirp, allowing mitigation of the power fading induced by chromatic dispersion for a given distance. (3) The chirp parameter has also impact on the maximum received power, through the factor ($1 + \alpha^2$).

In order to validate Eq. (12), Fig. 1 depicts the RF power of the received signal normalized by its maximum, obtained analytically from Eq. (12) and from numerical simulation of an OFDM-UWB signal following the ECMA-386 standard [16] centered at the frequency f_{rf} = 3.960 GHz, which corresponds to the 1st of 14 channels. The DEMZM is biased at the quadrature point. More details about the OFDM-UWB signal and the optical system parameters considered are provided in Section 3.

From Fig. 1 it is concluded that the analytical model derived for the signal photocurrent and its RF power shows excellent agreement with the numerical simulation results obtained, with a small discrepancy. This small discrepancy between the curves can be due to the high peak-to-average power ratio (PAPR) of the components $x_i(t)$ and $x_q(t)$. Hence, the approximation of the Bessel functions in Eq. (11) may not be accurate since $x_i(t)$ and $x_q(t)$ have high-peaks at some points. Furthermore, it is observed that the first null for $\alpha = -1$ occurs for a larger fiber length than for $\alpha = 0$.

2.2 Effect of DEMZM bias point on the modulation efficiency

For the small-signal analysis of the effect of DEMZM bias voltage on the optical powers and photodetected RF power, the DEMZM is considered without insertion losses, balanced (γ = 1), and the modulation is assumed chirpless ($\alpha = 0$). For these conditions, from Eq. (5) and Eq. (6), the power of the optical carrier is given by:

$$P_{OC} = \left(\frac{\sqrt{2P}}{2}\right)^2 |E_0|^2 = 4P\left(1+\cos\left(\frac{\pi}{V_\pi}\left(V_{bias1} + V_{bias2}\right)\right)\right), \quad (13)$$

and the average optical power of the signal sidebands is given by:

#196157 - $15.00 USD Received 20 Aug 2013; revised 4 Nov 2013; accepted 21 Nov 2013; published 6 Dec 2013

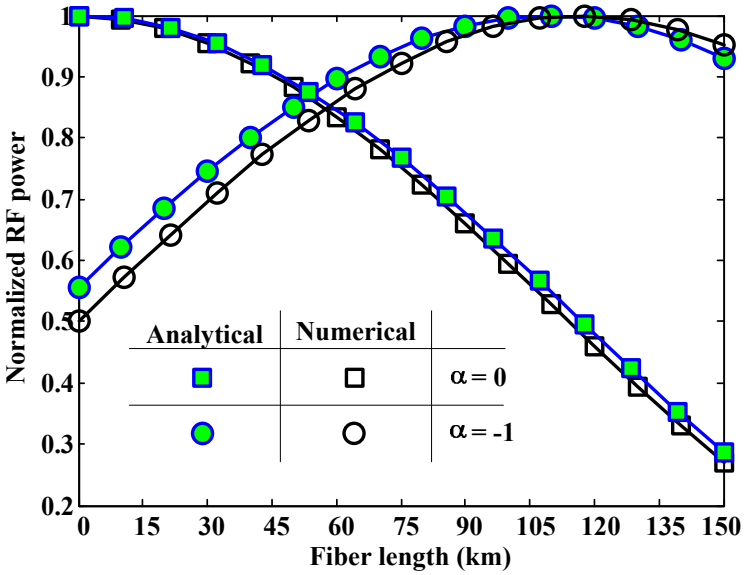

Fig. 1. Normalized RF powers as a function of fiber length, for an OFDM signal centered at 3.96 GHz.

$$P_{OSB} = \left(\frac{\sqrt{2P}}{2}\right)^2 \left\langle \left(|E_-|^2 + |E_+|^2\right)\right\rangle = 2\left(\frac{\sqrt{2P}}{2}\right)^2 \left\langle |E_+|^2 \right\rangle$$
$$= \frac{P}{2}(m\pi)^2\left(\sigma_{xi}^2 + \sigma_{xq}^2\right)\left(1 - \cos\left(\frac{\pi}{V_\pi}\left(V_{bias1} + V_{bias2}\right)\right)\right). \quad (14)$$

The RF power in optical B2B configuration, given by Eq. (11) for $L = 0$ and under the aforementioned conditions, can be rewritten taking into account the product of Eq. (13) by Eq. (14):

$$P_{rf} = R_L \Re^2 P_{OC} P_{OSB}. \quad (15)$$

Figure 2 depicts the optical power of the carrier, the optical power of the signal sidebands, the total optical power ($P_{OC} + P_{OSB}$) and the photodetected RF power, normalized by their maximum values, as functions of the bias voltage normalized by the half-wave voltage of the DEMZM. The normalized power of the optical carrier (P_{OC}) is equal to the intensity transfer function of an ideal DEMZM for negative bias voltages.

In Fig. 2 it can be observed that, when the bias voltage of the DEMZM decreases from the QP towards the MITP, the power of the optical carrier decreases whereas the optical power of the signal sidebands increases in the same proportion, and consequently the total optical power becomes dominated by the power of the signal sidebands.

Otherwise, when the bias voltage is increased from the QP towards the MATP, the power of the optical carrier increases and the total optical power is dominated by the carrier optical power. The performance and reach of the optical communication system are determined by P_{OSB}. By analogy with amplitude modulation in RF communication systems [17], the modulation efficiency is expressed by $\eta = P_{OSB}/(P_{OC} + P_{OSB}) \times 100$. Therefore, the efficiency reaches 100% if the optical carrier is totally suppressed, which requires the addition of an optical local oscillator at the receiver side to perform coherent detection. In direct detection systems, the most used systems in optical access networks, a fraction of the optical carrier must be transmitted to enable direct-detection. Therefore, the efficiency reaches 100% if the optical carrier is totally suppressed, which requires the addition of an optical local oscillator

#196157 - $15.00 USD Received 20 Aug 2013; revised 4 Nov 2013; accepted 21 Nov 2013; published 6 Dec 2013

at the receiver side to perform coherent detection. In direct detection systems, the most used systems

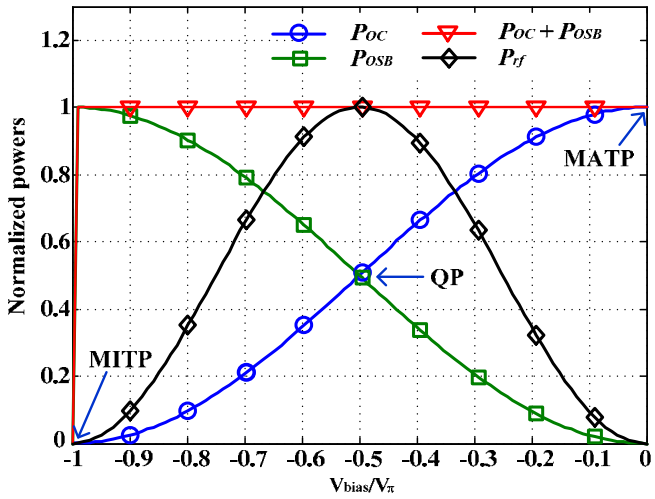

Fig. 2. Relationship between the optical powers and the RF power as functions of the V_{bias} voltage.

in optical access networks, a fraction of the optical carrier must be transmitted to enable direct-detection. Typically, the optimum performance is reached when the power of the optical carrier is reduced and equal to the optical power of the sidebands [4]. Therefore, with $P_{OC} = P_{OSB}$, the optimum modulation efficiency is 50% for direct-detection systems. Additionally, in Fig. 2 it can be observed that the maximum RF power is obtained when $P_{OC} = P_{OSB,}$ for the bias voltage equal to $-0.5V_{\pi}$, because the optical powers are normalized. Typically, at the output of the DEMZM biased at the QP, the power ratio between the optical carrier and the sidebands is approximately 20 dB [4].

3. Simulation setup

Figure 3 represents schematically a hybrid long-reach WDM-PON (LR-WDM-PON) for a single wavelength transmitted from the optical line terminal (OLT) located in the CO to the hybrid optical network unit/base station (ONU/BS) located at the customer's premises. In the CO, the optical transmitter based on the DEMZM has the modulation chirp controlled through the amplitudes of the drive signals [6].

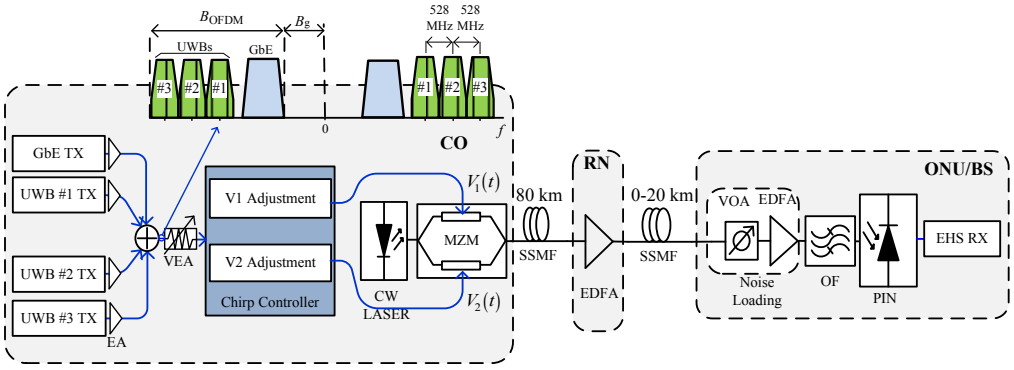

Fig. 3. Simulation transmission scheme of an OHS over a hybrid long-reach FTTH network with controlled modulation chirp.

#196157 - $15.00 USD Received 20 Aug 2013; revised 4 Nov 2013; accepted 21 Nov 2013; published 6 Dec 2013

An electrical hybrid signal (EHS) is created by subcarrier multiplexing four independent OFDM signals, a custom quadrature amplitude modulation (QAM) OFDM-Gigabit Ethernet (GbE) signal with 1 GHz bandwidth, and three independent quadrature phase shift keying (QPSK) OFDM-UWB signals following the ECMA-368 standard [16].

The three OFDM-UWB signals, UWB#1, UWB#2 and UWB#3, employing QPSK modulation with 528 MHz bandwidth, are up-converted to the frequencies 3.432, 3.960 and 4.488 GHz, respectively. These three channel signals perform no frequency hopping, with the three channels at time frequency codes (TFC) TFC5, TFC6 and TFC7, respectively. The subcarriers allocation in the OFDM-GbE signal is similar to the UWB signals. The OFDM-GbE signal is the unique that is not yet standardized, and thus can be freely translated in frequency, in order to maximize the guard band (B_g) between the DC frequency and the lower edge of the GbE signal spectrum and minimize the aggregate bandwidth of the OFDM signals (B_{OFDM}), as illustrated in Fig. 3. Thus, by allocating a guard band of 100 MHz between the GbE signal and the lower frequency UWB signal, the GbE signal is up-converted to the central frequency equal to 2.568 GHz, resulting in a B_{OFDM} = 2.684 GHz and a Bg = 2.068 GHz, which produce the ratio Bg/B_{OFDM} = 0.7705. Therefore, B_g is insufficient to accommodate all intermodulation distortion products generated upon direct-detection, since it has been shown that B_g should be at least equal to B_{OFDM} [18]. The main parameters used to generate the baseband OFDM signals used in the simulations are gathered in Table 1.

Table 1. Main Parameters Used to Generate the Baseband OFDM Signals

	GbE	**UWB1,2,3**
Nominal Bandwidth [MHz]	1000	528
Sampling frequency [MHz]	1056	528
FFT size (Total of subcarriers)	256	128
Data subcarriers	216	100
Pilot subcarriers	24	12
Guard subcarriers	15	10
Cyclic prefix [samples]	64	37*
Symbol time[μs]	0.303	0.312
Constellation mapping	QAM	QPSK
Central RF frequency[GHz]	2.568	3.432;3.960 and 4.488
Net bit rate [Mbit/s]	1425.7	641
References	~ [16]	[16]

*The cyclic prefix in the OFDM-UWB signals are null.

The EHS involving four separately amplified OFDM signals modulates externally a continuous wave (CW) laser with a linewidth of 5 MHz (conventional DFB laser) emitting at 1550 nm, through a DEMZM with 25 dB DC extinction ratio, half-wave voltage V_π = 5 V and 6 dB of insertion loss. The modulation index m is adjusted through a variable electrical attenuator (VEA). The model of the DEMZM is based on Eq. (2). The resulting OHS at the output of the DEMZM is transmitted through SSMF to the costumer's premises. The SSMF is modeled as the low-pass equivalent of a linear bandpass system. The SSMF is characterized by an attenuation of 0.22 dB/km and a chromatic dispersion parameter D = 17 ps/km/nm. After transmission through 80 km of SSMF, at the remote node (RN), the optical signal is amplified by a noiseless erbium doped fiber amplifier (EDFA) to compensate for the transmission losses. From the RN, the OHS is transmitted through fiber segments of length 0 km, 10 km and 20 km, to the hybrid ONU/BS located at the costumer's premises, in order to simulate the different locations of the customers relatively to the RN.

At the input of the hybrid ONU/BS, a variable optical attenuator (VOA) along with an EDFA are used to adjust the optical signal-to-noise ratio (OSNR) of the system, defined in a reference optical bandwidth of 0.1 nm. The OSNR is evaluated considering optical noise over the two perpendicular directions of polarization.

In the hybrid ONU/BS, a second-order super-Gaussian optical filter with 12.5 GHz full width at half maximum (FWHM) bandwidth, centered at 1550 nm, is used to reduce the amplified spontaneous emission (ASE) noise power, and a PIN photodetector with responsivity of 0.9 A/W is considered. The ASE noise is modeled as Gaussian noise. The

#196157 - $15.00 USD Received 20 Aug 2013; revised 4 Nov 2013; accepted 21 Nov 2013; published 6 Dec 2013

thermal noise of the receiver is not considered, since at the output of the PIN photodetector its effect is negligible, compared with the signal–ASE beating noise [19]. The received EHS is demodulated in the EHS receiver (EHS RX), where each OFDM signal is sent to the respective receiver to perform down-conversion and OFDM demodulation. The OFDM demodulation includes removal of cyclic prefix, serial-to-parallel conversion, FFT, subcarriers equalization, symbol de-mapping and parallel-to-serial conversion. The performance for each of the received OFDM signals is assessed through the required OSNR (ROSNR) for a bit error rate (BER) equal to 10^{-9}, estimated by the error vector magnitude (EVM) method applied to the constellation of the received signal at the equalizer output [20].

4. Numerical simulation results and discussion

The simulation results presented in this paper were produced with Matlab®, considering 528 OFDM-GbE symbols and 512 OFDM-UWB symbols. Since the OFDM signals have a spectrum similar to Gaussian noise and different bandwidths, the electrical power of each signal was adjusted for a power spectral density equal to −139.6 dB/Hz.

Initially, the optimum bias voltage of the DEMZM required to maximize the modulation efficiency of the system was investigated for an optical B2B configuration. The DEMZM was driven in balanced push-pull mode. In Fig. 4, contour plots of the ROSNR for a BER = 10^{-9} are shown as a function of the modulation index m for different values of the bias voltage normalized by the half-wave voltage of the DEMZM. Note that a BER = 10^{-9} is enough to ensure that the EVM limit of −14.5 dB after transmission, defined in the standard for QPSK OFDM-UWB signals, is respected.

Biasing the DEMZM below the QP, it operates in the non-linear region of its intensity transfer function, which degrades the transmitted signals due to the generation of harmonics and intermodulation distortion products. From Fig. 4, it can be concluded that the ROSNR can be kept constant when the DEMZM is biased below the QP, by decreasing m. The ROSNR for the UWB #2 signal shown in Fig. 4(c)) presents a degradation of nearly 2 dB relative to the UWB #1 and UWB #3 signals, due to linear crosstalk suffered from the adjacent channels. It can also be concluded that the lowest bias voltage of the DEMZM is limited by the GbE signal and is equal to $-0.8\ V_\pi$. Therefore, the optimum bias voltage equal to $-0.8V_\pi$ was selected to define the DSB-RC modulation, as the best value between all signals considered. In Fig. 5, the ROSNR is presented for all signals as a function of m when the DEMZM is biased at the QP, with $V_{bias} = -0.5V_\pi$, and below the QP, at $V_{bias} = -0.8V_\pi$.

Biasing the DEMZM at the QP, all signals present approximately the same ROSNR as m increases, whereas when the DEMZM is biased at $-0.8V_\pi$ the GbE and UWB #3 signals exhibit degradation relatively to the other signals, due to spurious spectral components resulting from the nonlinearity of the DEMZM transfer function and the square-law of the direct-detection. The GbE signal is degraded because the ratio B_g/B_{OFDM} is lower than 1, and thus a fraction of the GbE signal is distorted by intermodulation spectral components near DC, after photodetection. When the DEMZM is operated below the QP, the 2nd harmonic power of the GbE signal at 5.136 GHz increases, affecting the UWB#3 signal centered at 4.488 GHz. Furthermore, from Fig. 5 it is observed that the optimum values of m to drive the DEMZM are 0.35 and 0.45, for the DEMZM biased at $-0.8\ V_\pi$ and $-0.5\ V_\pi$, respectively. The average OSNR improvement of DSB-RC ($V_{bias} = -0.8V_\pi$) relative to DSB with full carrier ($V_{bias} = -0.5V_\pi$) for the optimum values of m, among all signals, is nearly 6 dB.

The drive voltage amplitudes expressed by Eq. (3) and Eq. (4) were derived from the small-signal approximation chirp parameter components presented in [11], and depend on the bias point of the DEMZM. Therefore, it is important to evaluate the accuracy of Eq. (3) and Eq. (4) for the optimum values of m obtained for different bias points of the DEMZM selected. The α chirp parameter value at the DEMZM output was measured as described in [11,21]. Figure 6 presents the absolute error between the desired α chirp parameter at the output of the DEMZM and the value obtained as a function of m, for the wired and wireless signals modulated in DSB-RC and DSB.

#196157 - $15.00 USD Received 20 Aug 2013; revised 4 Nov 2013; accepted 21 Nov 2013; published 6 Dec 2013

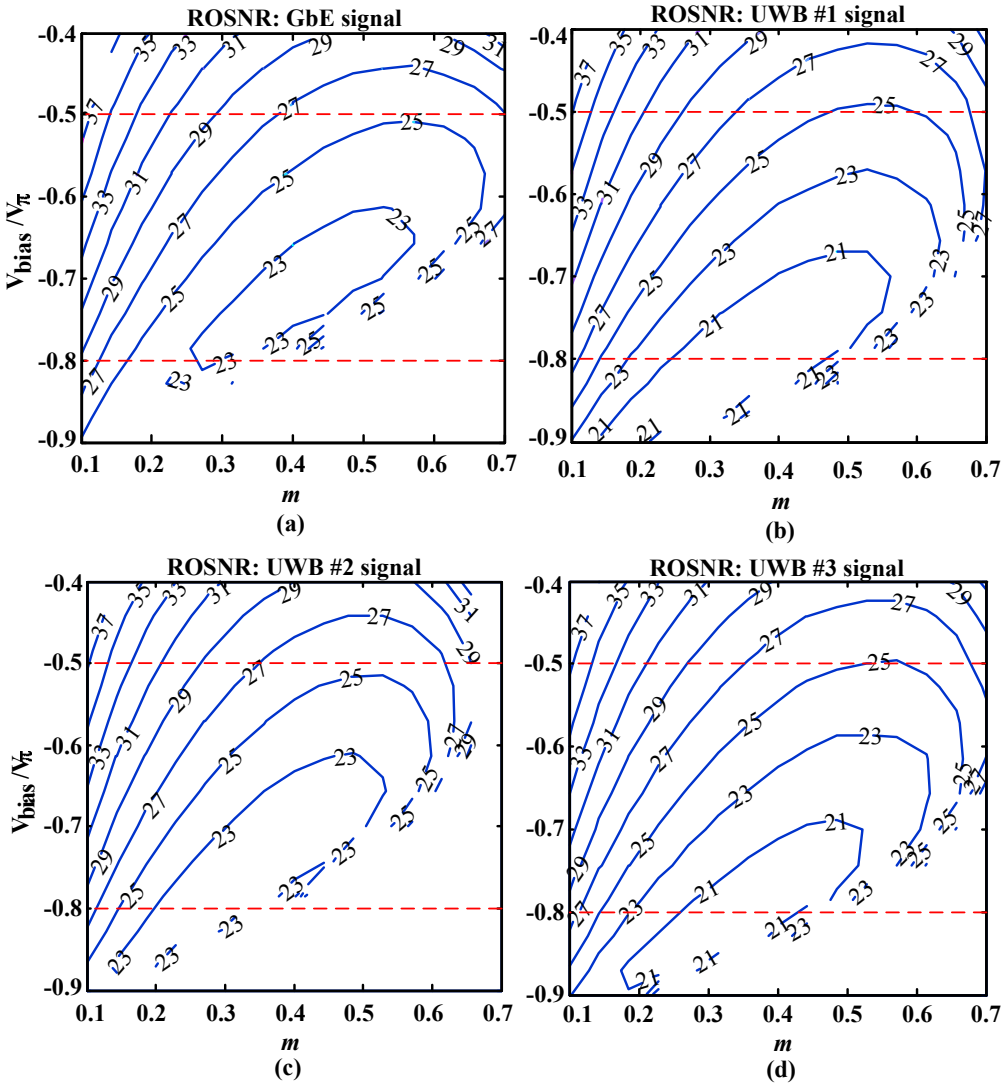

Fig. 4. Required OSNR for a BER = 10^{-9} as a function of the modulation index for different bias voltages, for: (a) OFDM-GbE signal; (b) OFDM-UWB #1 signal; (c) OFDM-UWB #2 signal; (d) OFDM-UWB #3 signal.

It can be concluded from Fig. 6 that, when the DEMZM is biased below its QP, the error of the α chirp parameter desired at the output of the DEMZM increases, relatively to the error with the DEMZM biased at the QP, due to the increase of the non-linearity of the DEMZM transfer function. Nevertheless, the values of the absolute error obtained for the two different bias voltages are negligible, within the range of values considered. Therefore, the modulation

#196157 - $15.00 USD Received 20 Aug 2013; revised 4 Nov 2013; accepted 21 Nov 2013; published 6 Dec 2013

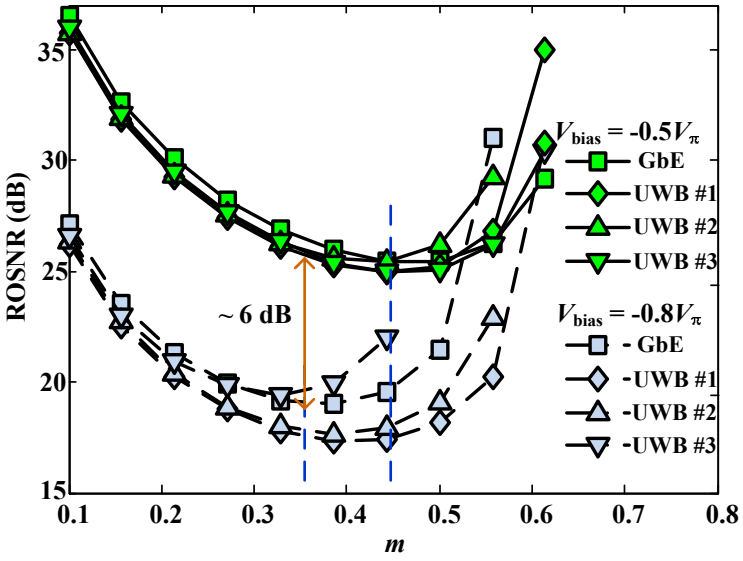

Fig. 5. Required OSNR for a BER = 10^{-9} as a function of the modulation index for two different bias point of DEMZM: $-0.5V_\pi$ and $-0.8V_\pi$.

chirp can be controlled with acceptable accuracy for both bias points selected.

In Section 2, the effects of the modulation chirp and bias point of a DEMZM on the received signal were analyzed separately. Now, the interaction of the two effects is assessed by numerical simulation.

The optimum α chirp parameter required to drive the DEMZM was studied for three different distances from the RN to the hybrid ONU/BS: 0, 10, and 20 km. These correspond to the distances of 80, 90 and 100 km from the OLT to the hybrid ONU/BS. In Fig. 7, the ROSNR is presented as a function of the α chirp parameter, for different distances from the CO to the hybrid ONU/BS with the GbE and UWBs signals modulated in DSB-RC and DSB.

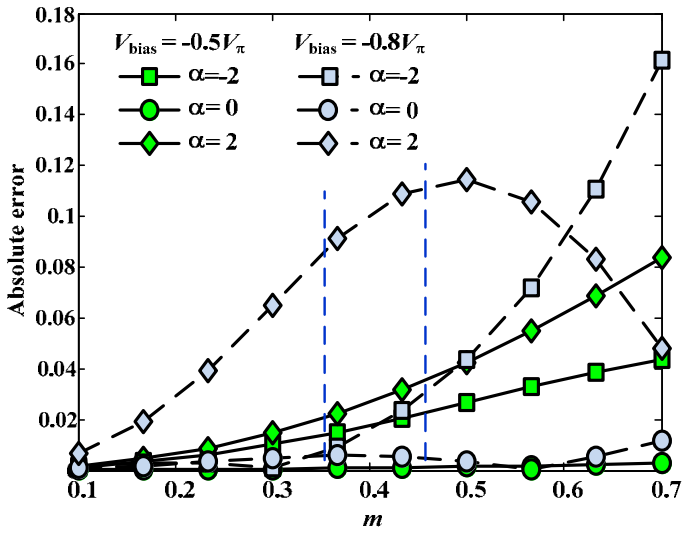

Fig. 6. Absolute error between the desired α chirp parameter at the output of the DEMZM and the value obtained for different bias points of the DEMZM: $-0.5V_\pi$ and $-0.8V_\pi$.

#196157 - $15.00 USD Received 20 Aug 2013; revised 4 Nov 2013; accepted 21 Nov 2013; published 6 Dec 2013

The DEMZM located in the OLT is driven at the optimum values of *m* selected from Fig. 5.

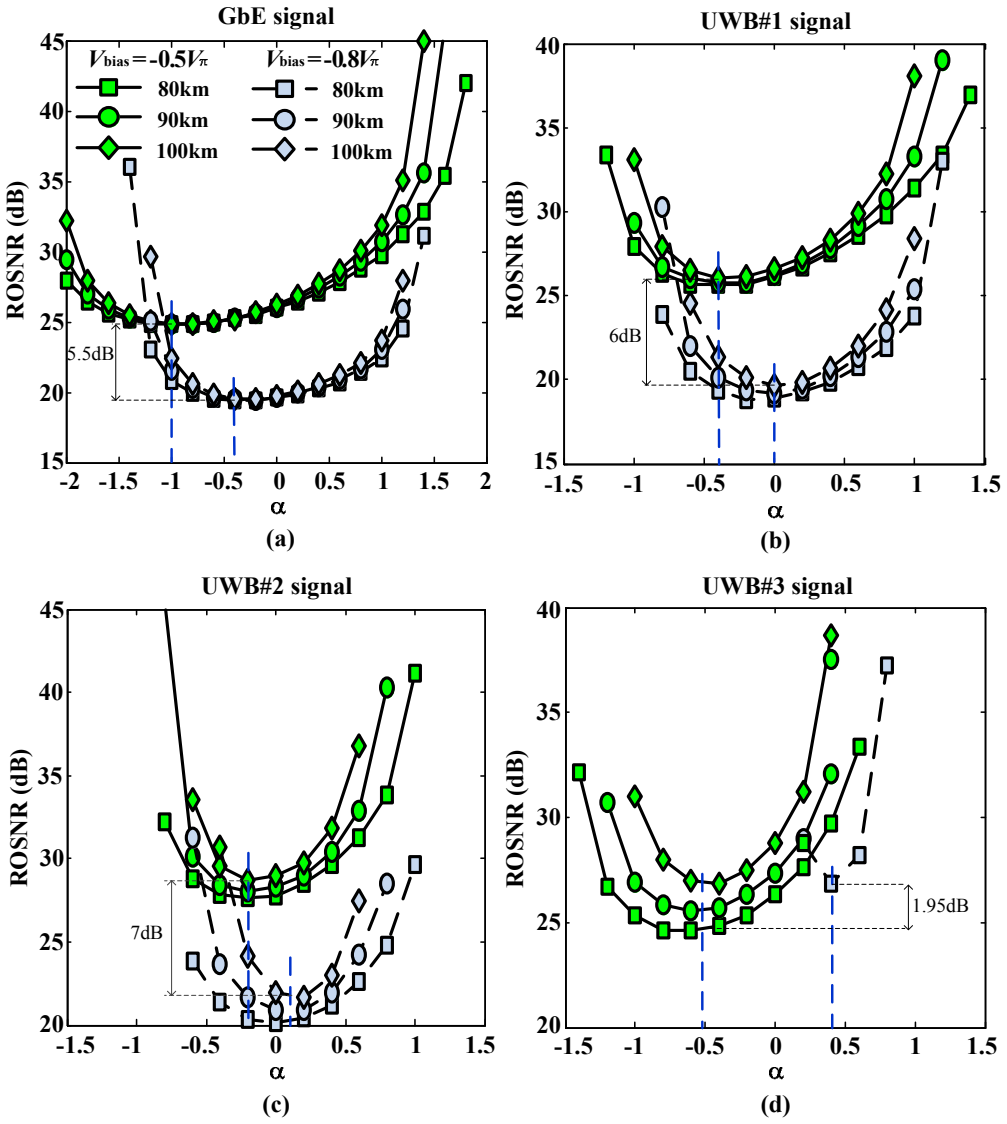

Fig. 7. Required OSNR for a BER = 10^{-9} for different distances from the CO to the ONU, as a function of the α chirp parameter, for the following signals: (a) GbE signal, (b) UWB#1 signal, (c) UWB#2 signal, (d) UWB#3 signal, modulated in DSB-RC ($V_{bias} = -0.8V_\pi$) and DSB ($V_{bias} = -0.5V_\pi$).

From Fig. 7 it is concluded that for DSB-RC modulation the introduction of controlled modulation chirp improves the performance for all signals, when compared with $\alpha = 0$. Furthermore, it is observed that, as the central frequency of the OFDM signals increases, the optimum values of α increase towards positive values, demonstrating that positive modulation chirp can also be useful to mitigate transmission dispersion penalty. On the other hand, for DSB modulation positive values of the α chirp parameter lead to additional dispersion penalty, whereas the negative values of α can mitigate the transmission dispersion penalty. Thus, it is concluded that the reduction of the optical carrier has impact on the optimum values of the α chirp parameter, moving them from negative to positive values. It is observed

#196157 - $15.00 USD Received 20 Aug 2013; revised 4 Nov 2013; accepted 21 Nov 2013; published 6 Dec 2013

that the benefits of the introduction of controlled modulation chirp, compared to $\alpha = 0$, are greater for DSB modulation than for DSB-RC modulation, mainly because the optimum values of α are more distant from $\alpha = 0$.

The ROSNR curves for the UWB#3 signal, shown in Fig. 7 d) for DSB-RC modulation, exhibit an OSNR degradation compared to DSB modulation, contrary to what is observed for the other OFDM signals. The reason for this is that the optimum value of the α chirp parameter for the UWB#3 signal modulated in DSB-RC is around 0.5, which unfortunately reduces the transmission bandwidth, and consequently the subcarriers of the UWB#3 signal are attenuated.

In order to understand the effect of the α chirp parameter on the transmission bandwidth, the frequency response for small-signal regime of a dispersive fiber link was derived considering as electro-optic modulator the DEMZM modeled by Eq. (2) and driven by the drive signals given by Eq. (3) and Eq. (4). To exclude the effects of the transmitter located in the OLT and of the receiver at the customer's premises, the frequency response given by Eq. (16) is normalized by the frequency response without optical fiber.

$$I_{sn}(f) = 2e^{-2\alpha_f}\sqrt{1+\alpha^2}\left|\cos\left[\frac{\pi D\lambda_c^2 f^2 L}{c} + \arctan(\alpha)\right]\right|, \qquad (16)$$

where α_f is the attenuation coefficient of the optical fiber. Equation (16) is similar to the equation presented in [22], derived for an electro-absorption modulator. Figure 8 shows the frequency response magnitude of a dispersive optical link, characterized by D = 17 ps/(km.nm), α_f = 0 dB/km and L = 100 km, for three different values of the α chirp parameter.

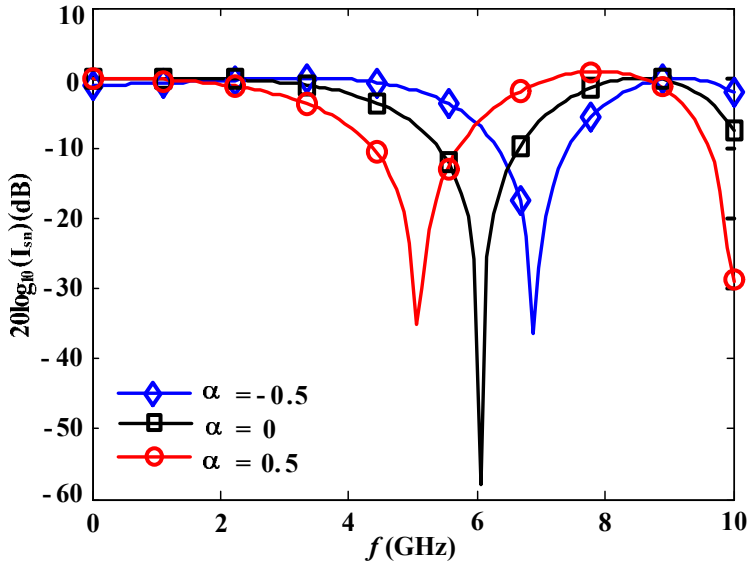

Fig. 8. Frequency response magnitude of a dispersive optical link.

From Fig. 8, it is observed that for $\alpha = 0$ the first null in the frequency response occurs around 6 GHz, for $\alpha = -0.5$ around 6.9 GHz, and for $\alpha = 0.5$ around 5 GHz. Thus, for $\alpha = 0.5$ the transmission bandwidth is reduced approximately 1 GHz compared to $\alpha = 0$. The null in the frequency response around 5 GHz for $\alpha = 0.5$ attenuates the subcarriers of the UWB#3 signal centered at 4.488 GHz and with 528 MHz bandwidth, which justifies the OSNR degradation observed in Fig. 7(d)) for DSB-RC relative to DSB modulation. However, this problem can be overcome by changing adaptively the power of the different OFDM signals, using a centralized frequency response compensation approach located at the optical line terminal (OLT), such as proposed in [23]. This issue shall be addressed in future work.

#196157 - $15.00 USD Received 20 Aug 2013; revised 4 Nov 2013; accepted 21 Nov 2013; published 6 Dec 2013

5. Conclusions

The α chirp parameter of a LiNbO3 DEMZM does not depend on the average optical power at its output. This characteristic was exploited in this paper, in order to control the modulation efficiency and modulation chirp of a DEMZM independently. A performance comparison between DSB and DSB-RC modulations, based on the ROSNR for a BER = 10^{-9} for different values of the modulation chirp parameter, was carried out by numerical simulation and it was demonstrated that the introduction of controlled modulation chirp is more advantageous for DSB modulation than for DSB-RC modulation, because the reduction of the optical carrier power has the effect of moving the optimum value of the α chirp parameter closer to $\alpha = 0$. Furthermore, it was demonstrated that the optimum value of the α chirp parameter increases towards positive values as the central frequency of the OFDM signal increases, enabling positive modulation chirp to mitigate the transmission dispersion penalty.

Finally, the control of the DEMZM bias point and modulation chirp can be exploited to improve the transmission performance of the future hybrid optical access networks.

Acknowledgments

This work was supported by the Portuguese Foundation for Science and Technology, through the PhD grant SFRH/BD/62647/2009 and the project PEst-OE/EEI/LA0008/2013.

#196157 - $15.00 USD Received 20 Aug 2013; revised 4 Nov 2013; accepted 21 Nov 2013; published 6 Dec 2013